NanoImpact 14 (2019) 100152

Contents lists available at ScienceDirect

NanoImpact

journal homepage: www.elsevier.com/locate/nanoimpact

Research paper

# Multi-walled carbon nanotubes inhibit estrogen receptor expression *in vivo* and *in vitro* through transforming growth factor beta1

L. Cody Smith[a,b], Santiago Moreno[b], Sarah Robinson[b,e], Marlene Orandle[c], Dale W. Porter[c], Dipesh Das[d], Navid B. Saleh[d], Tara Sabo-Attwood[b,e,*]

[a] Department of Physiological Sciences, University of Florida, Gainesville, FL, USA
[b] Center for Environmental and Human Toxicology, University of Florida, Gainesville, FL, USA
[c] National Institute for Occupational Safety and Health, Health Effects Laboratory Division, Morgantown, WV 26505, USA
[d] Department of Civil, Architectural and Environmental Engineering, The University of Texas at Austin, Austin, TX, USA
[e] Department of Environmental and Global Health, University of Florida, Gainesville, FL, USA

ARTICLE INFO

*Keywords:*
Multi-walled carbon nanotube
Transforming growth factor beta1
Estrogen receptor
Lung

ABSTRACT

Exposure to multi-walled carbon nanotubes (MWCNTs) is suspected to contribute to pulmonary fibrosis through modulation of transforming growth factor beta1 (TGF-β1). There is growing evidence that estrogen signaling is important in pulmonary function and modulates pro-fibrogenic signaling in multiple models of pulmonary fibrosis, however an interaction between MWCNT exposure and estrogen signaling in the lung is not known. The purpose of this work was to determine whether estrogen signaling in the lung is a target for MWCNTs and to identify potential signaling mechanisms mediating MWCNT-induced responses using a whole-body inhalation mouse model and an *in vitro* human lung cell model. Mice exposed to MWCNTs had reduced mRNA expression of estrogen receptor alpha and beta (*Esr1* and *Esr2*, respectively) in lung tissue at multiple time-points post exposure, whereas expression of G-protein coupled estrogen receptor 1 (*Gper1*) was more variable. We localized ESR1 protein expression as primarily associated with bronchioles and within inflammatory macrophages. The reduction in estrogen receptor expression was concomitant to an increase in TGF-β1 levels in the bronchoalveolar lavage fluid (BALF) of MWCNT-exposed animals. We confirmed a role for TGF-β1 in mediating MWCNT-induced repression of *ESR1* mRNA expression using a TGF-β type-I receptor inhibitor in bronchial epithelial cells *in vitro*. Overall these results highlight a novel mechanism of MWCNT-induced signaling where MWCNT-induced regulation of TGF-β1 represses estrogen receptor expression. Dysregulated estrogen signaling through altered receptor expression may have potential consequences on lung function.

## 1. Introduction

Multi-walled carbon nanotubes (MWCNTs) are concentric graphene tubes with a diameter < 100 nm, high aspect ratio, and unique physiochemical and electro-conductive properties (De Volder et al., 2013). The unique properties of MWCNTs make them appealing for a variety of applications in electronics, engineering, manufacturing, and medicine (Endo et al., 2008). Their widespread application and increased use each year enhances the potential for human exposure through occupational, environmental, medical, and consumer routes (Vietti et al., 2016). There is concern for adverse pulmonary effects occurring through inhalation due to the high aspect ratio of MWCNTs (Donaldson

*Abbreviations:* ACTB, beta-actin; BALF, bronchoalveolar lavage fluid; BEAS-2Bs, bronchial epithelial cells; BEBM, bronchial epithelial basal medium; BEGM, bronchial epithelial growth medium; BPE, bovine pituitary extract; Col1a1, collagen type 1 alpha 1 chain; Col1a2, collagen type 1 alpha 2 chain; DCFDA, 2′,7′-dichlorofluorescin diacetate; DMSO, Dimethyl sulfoxide; DPPC, dipalmitoylphosphatidylcholine; E2, 17β-estradiol; ECM, extracellular matrix; ELISA, enzyme-linked immunosorbent assay; ESR1, estrogen receptor alpha; ESR2, estrogen receptor beta; Fn1, fibronectin; GAPDH, glyceraldehyde phosphate dehydrogenase; GPER1, G-protein coupled estrogen receptor; HDR, hydrodynamic radius; IHC, immunohistochemistry; IPF, idiopathic pulmonary fibrosis; MIQE, minimum information for publication of qPCR experiments; MWCNT, multi-walled carbon nanotube; PAS, periodic acid-Schiff; PSN, Penicillin-Streptomycin-Neomycin; qPCR, Quantitative Real-Time Polymerase Chain Reaction; ROS, reactive oxygen species; TBRI, transforming growth factor beta receptor type 1; TGF-β1, transforming growth factor beta1; TRDLS, time-resolved dynamic light scattering

* Corresponding author at: Department of Environmental and Global Health, Center for Environmental and Human Toxicology, University of Florida, Box 110885, 2187 Mowry Rd., Gainesville, FL 32611, USA.
*E-mail address:* sabo@phhp.ufl.edu (T. Sabo-Attwood).

https://doi.org/10.1016/j.impact.2019.100152
Received 7 January 2019; Received in revised form 8 March 2019; Accepted 19 March 2019
Available online 21 March 2019

et al., 2013).

Animal studies have indicated that MWCNTs cause respiratory toxicity including inflammatory changes, lung remodeling and fibrosis, mesothelioma, and promotion of lung adenocarcinoma (Muller et al., 2005; Poland et al., 2008; Ryman-Rasmussen et al., 2009a; Sargent et al., 2014). The pro-fibrotic potential of MWCNTs is underscored by the measurement of fibrotic biomarkers in the blood of workers in MWCNT manufacturing plants (Fatkhutdinova et al., 2016). In animals, MWCNTs have been shown to cause acute dose-dependent fibrotic-like changes in the lung, evidenced by excess collagen deposition in foci of inflammation, upregulation of the pro-fibrogenic cytokine, transforming growth factor beta1 (TGF-β1), and induction of fibrotic marker gene expression such as collagen 1 (*Col1a1*), collagen 2 (*Col1a2*), and fibronectin (*Fn1*) in mice (Porter et al., 2012; Dong et al., 2015; Wang et al., 2015). MWCNT-induced pulmonary fibrosis has been observed to persist up to 336 days post exposure in mice (Mercer et al., 2013).

There is growing evidence supporting a role for sex hormones, particularly estrogen (E2) in lung function and disease (Carey et al., 2007a, 2007b; Tam et al., 2011; Townsend et al., 2012; Shim et al., 2013; Sathish et al., 2015). While a link between MWCNTs and other particles and fibers to pulmonary fibrosis has been documented, few studies have investigated whether estrogen-mediated pathways through cognate receptors are targets of MWCNT exposure in the lung. One mechanism could be through altering the expression of estrogen receptors yet only a handful of studies have investigated such changes in response to particulates. For example, one study found that intratracheal instillation of silica nanoparticles to male and female mice significantly reduced mRNA expression of the nuclear estrogen receptors (*Esr1* and *Esr2*) but not the membrane-bound G-protein coupled estrogen receptor (*Gper1*) in the lung after 14 days (Brass et al., 2010). A more recent study by our group reported that exogenous administration of TGF-β1 caused reduced expression of *ESR1*, *ESR2*, and *GPER1* mRNA expression in bronchial epithelial cells (BEAS-2Bs) (Smith et al., 2018) highlighting the potential link between ESRs and pro-fibrotic signaling pathways. It is possible that such mechanisms contribute to noted sex differences in the incidence and severity of pulmonary fibrosis. Data from epidemiological studies indicate that pulmonary fibrosis is more common in men, and that women have better survival rates (Gribbin et al., 2006; Han et al., 2008), however, results from studies investigating a role for sex steroid signaling in animal models have been mixed. For example, male mice exhibited greater fibrosis than female mice after treatment with the chemotherapeutic bleomycin (Voltz et al., 2008; Redente et al., 2011), whereas estrogen (17β-Estradiol, E2) supplementation exacerbated bleomycin-induced fibrosis in female rats (Gharaee-Kermani et al., 2005). These discrepancies highlight a need for foundational data that improve our understanding of how known fibrogenic and sex steroid signaling mechanisms may interface and influence each other (or not).

To determine whether estrogen signaling is modulated in particulate-induced lung disease, we sought to probe interactions between pro-fibrogenic and estrogen receptor signaling mechanisms using both *in vivo* and *in vitro* models of MWCNT exposure. E2 exerts its effects by binding and activating several receptors including the nuclear transcription factors ESR1 ESR2, and several variants thereof (Gruber et al., 2002), and the membrane-bound GPER1 (Filardo et al., 2002; Prossnitz et al., 2008). Herein, we investigated the effect of MWCNT exposure on estrogen receptor expression in the lung as a surrogate for E2 signaling in human lung epithelial cells *in vitro* and mouse lung tissues that show inflammation and pro-fibrotic histopathological changes.

## 2. Materials and methods

### 2.1. Chemicals

Two types of MWCNTs were used in this study including MWCNT-7 from Mitsui & Co., Ltd. Tokyo, Japan referred to here as Mitsui MWCNTs and another particle from Helix Materials Solutions, Inc., Richardson, Texas, USA referred to as Helix MWCNTs. The Selective inhibitor of TGF-β type-I receptor, LY 364947 (purity: > 99%) was purchased from Tocris Bioscience, Bristol, UK (Cat. No. 2718) and dissolved in Corning™ cellgro™ dimethyl sulfoxide (DMSO, Corning™ 25950CQC, Thermo Fisher Scientific, Waltham, MA), final solvent concentration < 0.1%. Bovine serum albumin (BSA) was purchased from Fisher Scientific Co LLC (BP1605, Pittsburgh, PA) and 1,2-Dipalmitoyl-sn-glycero-3-phosphocholine (purity: ≥99%) (DPPC) was purchased from Sigma (P0163, Saint Louis, MO).

### 2.2. Animal exposure

The mouse inhalation exposure study was performed at NIOSH and has been described previously (Porter et al., 2012). Briefly, Male C57BL/6J mice (6 weeks old) were exposed to a Mitsui MWCNT aerosol (10 mg/m$^3$, 5 h/day) for either 2, 4, 8, or 12 days. At one day post-exposure, bronchoalveolar lavage (BAL) was collected by inserting a cannula into the trachea and instilling 1 mL ice-cold $Ca^{2+}$ and $Mg^{2+}$-free PBS, pH 7.4, supplemented with 5.5 mM D-glucose. Recovered BAL was subsequently stored at −80 °C. From separate sets of mice, lungs were removed and fixed for histopathology.

### 2.3. Histopathology

At necropsy, lungs were inflated with 6 cc of 10% formalin and processed into paraffin blocks. Formalin-fixed and paraffin-embedded tissue blocks were cut at 5 μm and mounted on non-coverslipped slides. H&E staining, Masson's Trichrome staining, and Alcian-Blue/PAS staining was performed by Histology Tech Services (Gainesville, FL).

### 2.4. Enzyme-linked immunosorbent assay (ELISA)

Bronchoalveolar lavage samples (BALF) from mice exposed to clean air or Mitsui MWCNT aerosol (5 mg/m$^3$, 5 h/day) for 4 days were centrifuged for 20 min at 14,000 ×*g* at 4 °C, and 100 μL of the supernatant was removed for TGF-β1 quantification using the Quantikine® ELISA kit from R&D Systems (MB100B, Minneapolis, MN). Latent TGF-β1 was activated by adding 20 μL of 1 N HCl to 100 μL supernatant, vortexing, and incubating for 10 min at room temperature. The reaction was neutralized by adding 20 μL of 1.2 N NaOH/0.5 M HEPES and vortexing. Active TGF-β1 was quantified per manufacturer's recommendations.

### 2.5. Immunohistochemistry (IHC)

Formalin-fixed, paraffin embedded tissues were sectioned at 5 μm and placed on charged slides. Prepared slides were then deparaffinized in xylenes and rehydrated through graded concentrations of ethanol. Antigen Masking Solution (Vector Labs, Burlingame, CA) was used to regain antigenicity. Slides were blocked for 30 min (Dako Serum Free Block, (Dako, Santa Clara, CA) and then incubated in primary antibody, Anti-Estrogen Receptor alpha (AB75635, ABCAM Cambridge, MA) for 1 h. The primary antibody was diluted 1:100 with Dako Diluent (Dako, Santa Clara, CA). Negative and positive control slides were included. Negative control slides were incubated in diluent. Slides were rinsed with PBS (Sigma, St Louis, MO) and incubated for 30 min with biotinylated goat anti rabbit secondary antibody diluted 1:200 (Vector, Burlingame, CA). Slides were rinsed and then incubated for 30 min with Elite ABC Kit (Vector, Burlingame, CA). Slides were developed with DAB substrate (Sigma, St. Louis, MO) for 90 s and counterstained in Mayer's Hematoxylin (Sigma, St. Louis, MO). All incubations were performed in a humidity chamber at room temperature.

### 2.6. Cell culture

Human bronchial epithelial cells (BEAS-2Bs, CRL-9609™) were purchased from ATCC and cultured per the manufacturer's specifications. Cells were cultured in bronchial epithelial growth medium (BEGM) consisting of bronchial epithelial basal medium (BEBM, Lonza CC-3171, Walkersville, MD) and the BEGM SingleQuot Kit Supplements & Growth Factors (Lonza CC-4175), replacing gentamicin with 1% Penicillin-Streptomycin-Neomycin (PSN) Antibiotic Mixture (Gibco 15640, ThermoFisher Scientific Inc.). Cells were cultured in T75 Corning™ U-Shaped Cell Culture Flasks (Corning 430641 U, Fisher Scientific Co LLC) coated with a matrix (4.5 mL per 75 $cm^2$) consisting of 0.01 mg/mL fibronectin (Akron AK8350, Boca Raton, FL), 0.03 mg/mL bovine collagen (Gibco A10644-01, ThermoFisher Scientific Inc.), and 0.01 mg/mL BSA (Fisher BP1605, Fisher Scientific Co LLC) in BEBM. All exposures were performed in BEGM without the supplied bovine pituitary extract (BPE) aliquot because its composition is not defined. For the gene expression experiments, BEAS-2Bs were plated at 40,000 cells/mL on matrix-coated 12-well Nunc™ Cell-Culture Treated Multidishes (ThermoFisher Scientific Inc., 150628), allowed to adhere overnight, and subsequently exposed for 48 h to the indicated concentrations of MWCNTs.

### 2.7. Nanotube dispersion and characterization in vitro

For *in vitro* experiments, stock solutions of Mitsui MWCNTs were dispersed based on the method described by Porter et al. (Porter et al., 2008). Briefly, Mitsui MWCNTs were suspended in dispersion media ($Ca^{2+}$- and $Mg^{2+}$-free phosphate buffered saline, pH 7.4, supplemented with 0.6 mg/mL BSA and 0.01 mg/mL DPPC) at 2 mg/mL. The MWCNT stock was sonicated in a water bath sonicator (Branson B-220) for 10 min, then sonicated using a Branson 450 Sonifier fitted with a 1/8-inch tip in an ice bath at 50% amplitude for 10 min with an 8 s pulse and 10 s rest between pulses. Stock solutions of Helix MWCNTs were prepared based on the method described by Wang et al. (Wang et al., 2010). Briefly, Helix MWCNTs were suspended in ultrapure water at 5 mg/mL and sonicated using the same parameters as for the Mitsui MWCNT dispersion. Both MWCNT stock solutions were dispersed at the concentrations indicated in the manuscript in BEGM without BPE supplemented with 0.6 mg/mL BSA and 0.01 mg/mL DPPC.

Time dependent hydrodynamic radii (HDR) of both Helix (Supplementary Fig. 3A) and Mitsui (Supplementary Fig. 3B) MWCNTs were monitored with time resolved dynamic light scattering (TRDLS). A 22 mW 632 nm HeNe laser incorporated ALV/CGS-3 compact goniometer system (ALV-Laser GmbH, Langen/Hessen, Germany) with QE APD detector (photomultipliers of 1:25 sensitivity) was employed to monitor size evolution every 15 s for 48 h. The TRDLS experiments were performed at 37 °C for both samples with 2 mL of sample in a borosilicate glass vial, which was cleaned thoroughly with 2% Dextran solution. These vials were vortexed for 10 s before inserting in the toluene-filled sample vat of the goniometer system. The scattered light was collected at 90° and analyzed using an auto cross-correlator to calculate average HDR.

The electrophoretic mobility (EPM) of both MWCNT suspensions were measured using a Mobius (Wyatt Technology, Santa Barbara, CA) at 25 °C and 30 psi (Supplementary Fig. 3C). For each measurement, 1 mL of the MWCNT suspension was introduced into a flow-through cell using a 1 mL syringe. Five EPM values were collected for each of the MWCNT suspensions. The cells were washed with deionized water and ethanol between measurements.

### 2.8. Total RNA extraction and purification

Total RNA was extracted from whole lung and cell lysates using RNA STAT-60™ Reagent (Tel-Test, Inc. Cs-502, Friendswood, TX). Cell lysates were vortexed and whole lung tissue was mechanically disrupted. Total RNA was extracted per manufacturer's specifications. RNA was precipitated overnight at −20 °C in 100% molecular biology grade isopropanol (Fisher BioReagents™ BP26184, ThermoFisher Scientific Inc.) containing 0.067% GlycoBlue™ Coprecipitant (Ambion® AM9515, ThermoFisher Scientific Inc.) and purified by washing 2× with 75% molecular biology grade absolute ethanol (Fisher BioReagents™ BP28184, ThermoFisher Scientific Inc.). RNA pellets were reconstituted in 15 µL RNAsecure™ (Ambion® AM7010, ThermoFisher Scientific Inc.). RNA was quantified using a Synergy™ H1 plate reader (BioTek Instrument, Inc., Winooski, VT) and RNA integrity was spot-checked using a Bioanalyzer 2100 instrument (Agilent Technologies, Santa Clara, CA).

### 2.9. Quantitative real-time polymerase chain reaction (qPCR)

Total RNA was DNase-treated using the PerfeCTa DNase I Kit (Quanta BioSciences 95150-01 k, VWR International LLC, Suwanee, GA) and DNase-treated RNA was subsequently reverse transcribed using the qScript™ cDNA Synthesis Kit (Quanta BioSciences 95047, VWR International LLC). cDNA was diluted 1:20 in RNase-DNase free water. Each 10 µL qPCR reaction contained 1× SsoAdvanced™ Universal SYBR® Green Supermix (Bio-Rad 172-5270, Hercules, CA), 850 nM forward and reverse primers, and 3.3 µL of the cDNA dilution. Gene specific primers and cycling parameters are displayed in Table 1. Each qPCR reaction was followed by melt curve analysis to verify primer specificity. Cq values were determined by regression method using the CFX Manager 2.1 software and quantified using the relative ΔΔCq method (Hellemans et al., 2007) or the ratio method (Pfaffl, 2001) where indicated. Target gene expression was normalized to glyceraldehyde 3-phosphate dehydrogenase (*GAPDH*) expression.

### 2.10. Intracellular reactive oxygen species (ROS) measurement

Intracellular ROS was measured using the DCFDA Cellular ROS Detection Assay kit (abcam®ab113851, Cambridge, UK). BEAS-2Bs were plated at 30,000 cells per well on matrix-coated black wall, clear bottom 96-well plates (Corning 3603, Fisher Scientific Co LLC) and allowed to adhere overnight. Once cells reached 90% confluency, they were washed with 1× Buffer, then stained with 20 mM DCFDA dye for 45 min at 37 °C in the dark. Thereafter, DCFDA solution was removed,

**Table 1**
Primer details for qPCR.

| Gene | Forward (5′-3′) | Reverse (5′-3′) | Protocol | Efficiency (%) | Source |
|---|---|---|---|---|---|
| *GAPDH* | GAAGGTGAAGGTCGGAGTC | GAAGATGGTGATGGGATTTC | 95C 3 m; 95C 10s, 60C 30s, x40 | 93.9 | (Beck et al., 2006) |
| *ESR1* | CCACCAACCAGTGCACCATT | GGTCTTTTCGTATCCCACCTTTC | 95C 3 m; 95C 10s, 60C 30s, x40 | 100.7 | (Spizzo et al., 2010) |
| *ESR2* | Proprietary | Proprietary | 95C 3 m; 95C 10s, 60C 30s, x40 | 102.9 | Bio-Rad |
| *GPER1* | GCTCCCTGCAAGCAGTCTTT | GAAGGTCTCCCCGAGAAAGC | 95C 3 m; 95C 10s, 60C 30s, x40 | 97.2 | (Ye et al., 2012) |
| *Gapdh* | AGGTCATCCCAGAGCTGAACG | CACCCTGTTGCTGTAGCCGTAT | 95C 3 m; 95C 10s, 58C 10s, 72C 30S, x40 | 91.9 | (Ha et al., 2010) |
| *Esr1* | GGAAGCTCCTGTTTGCTCCT | AACCGACTTGACGTAGCCAG | 95C 3 m; 95C 10s, 62C 30s, x40 | 95.1 | (Ye et al., 2012) |
| *Esr2* | CGCAGACGAAGAGTGCTGT | AGCCAAGGGGTACATACTGG | 95C 3 m; 95C 10s, 60C 30s, x40 | 98.7 | (Ye et al., 2012) |
| *Gper1* | CAGTCTTTCCGTCACGCCTA | GCTCGTCTTCTGCTCCACAT | 95C 3 m; 95C 10s, 60C 30s, x40 | 91.8 | (Ye et al., 2012) |

and the cells were washed with 1 × PBS. The washed cells were exposed to increasing concentrations of MWCNTs for 6 h and fluorescence was measured at Ex/Em = 485/535 nm.

### 2.11. Statistics

Normality of experimental data was determined by D'Agostino & Pearson omnibus normality test, Shapiro-Wilk normality test, and KS normality test using GraphPad Prism software (Version 5.01, GraphPad Software, Inc., La Jolla, CA). Data were determined to be normal by passing at least one normality test ($p < 0.05$). If the data were normal, significant differences ($p < 0.05$) in means were determined by one-way ANOVA followed by Newman-Keuls multiple comparison test or one-tailed unpaired *t*-test using GraphPad Prism 5.01 software. Outliers were identified using Grubbs' test using the following website: https://www.graphpad.com/quickcalcs/grubbs2/.

## 3. Results

### 3.1. Mitsui MWCNTs cause histopathological alterations in the lungs of mice

The histopathological alterations observed in this study were reported in full detail elsewhere (Porter et al., 2012) and re-evaluated here in independent samples. Briefly, the lungs of exposed animals exhibited inflammation centered at the bronchioalveolar duct junction, hyperplasia and hypertrophy of the bronchiolar epithelium, airway mucous metaplasia, fibrosis, and vascular changes (Porter et al., 2012). For the present study, new slides from the same MWCNT inhalation study were prepared and confirmed that bronchiolar epithelial cell hypertrophy and hyperplasia was present in all Mitsui MWCNT-exposed mice at all time points (Supplementary Fig. 1B-D). Lung fibrosis was minimal to mild in severity as indicated by a subtle increase in collagen staining in the lungs of mice exposed to Mitsui MWCNTs for 8 and 12 days (Supplementary Fig. 1G-H). Prominent mucous metaplasia was apparent in mice exposed to Mitsui MWCNTs for 8 and 12 days and was primarily seen in small bronchioles as evidenced by heavy magenta staining of the airway epithelium (Supplementary Fig. 1K-L).

### 3.2. Measurement of TGF-β1 levels in BALF of mice exposed to Mitsui MWCNTs

MWCNTs have been shown to increase total TGF-β1 levels in the BALF of mice (Wang et al., 2011; Ronzani et al., 2012; Li et al., 2013; Wang et al., 2013; Chen et al., 2014; Dong et al., 2015), so we investigated whether a similar response occurred in our model. It should be noted that that we were not able to obtain BALF samples from mice exposed to 10 mg/m$^3$ MWCNTs, but were able to quantify total TGF-β1 in the BALF of mice exposed to clean air or 5 mg/m$^3$ Mitsui MWCNTs for 5 h per day at 4 days post exposure that were collected from a parallel study. TGF-β1 levels were quantified by ELISA. The mean ± SEM of TGF-β1 levels in control and Mitsui MWCNT-exposed mice were 86.67 ± 14.92 ($n = 6$) and 110.5 ± 6.83 ($n = 7$), respectively. There was an increased trend in levels of TGF-β1 however these levels were not quite statistically significant from controls as determined by one-tailed, unpaired *t*-test ($p = 0.0776$) (Fig. 1).

### 3.3. Mitsui MWCNTs reduce estrogen receptor mRNA expression in mouse lungs

Previous data has shown that TGF-β1 reduces ESR1 mRNA and protein expression *in vitro* in bronchial epithelial cells (Smith et al., 2018), so we questioned whether the increased trend of BALF TGF-β1 levels were associated with changes in estrogen receptor expression *in vivo* in the lungs of mice exposed to Mitsui MWCNTs. In an effort to reuse and reduce the use of animals in our research, we began

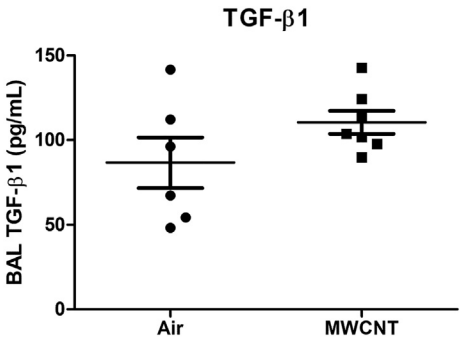


**Fig. 1.** Mitsui MWCNTs upregulate TGF-β1 levels in bronchoalveolar lavage fluid (BALF). Mice were exposed to clean air or 5 mg/m$^3$ aerosolized MWCNTs for 5 h per day for 4 days and TGF-β1 levels were determined in BALF by ELISA. Each point represents TGF-β1 level in one mouse. Lines indicate mean ± SEM. Asterisk (*) indicates statistically significant differences between means ($p = 0.0776$) as determined by one-tailed, unpaired *t*-test.

investigations on male mice exposed to MWCNTs in a former study. These studies are relevant in light of previous studies which indicated that exposure to another particulate (silica) resulted in reduced expression of *Esr1* and *Esr2* in lungs of male mice (Brass et al., 2010). Furthermore, the goal of this study was to observe the connection between pro-fibrotic and steroid pathways, not to perform a comparison in injury between males and females at this point. We evaluated mRNA expression of *Esr1*, *Esr2*, and *Gper1* by qPCR in whole lung lysates of mice obtained 1 day after exposure for 2, 4, 8, or 12 days to clean air or 10 mg/m$^3$ Mitsui MWCNTs by whole-body inhalation for 5 h per day. The expression levels of *Esr1*, *Esr2*, and *Gper1* in lungs of mice exposed to clean air for 2 days were expressed as a ratio to *Esr2* based on the method described by Pfaffl et al. (Pfaffl, 2001) to determine relative baseline expression. The relative basal expression level of each receptor subtype was *Gper1* > *Esr1* > *Esr2* (Fig. 2A).

For the time-course analysis, fold changes for all samples were calculated relative to expression levels in lungs of mice exposed to clean air for 2 days. The relative expression of each receptor subtype varied over the time-course in both clean air- and Mitsui MWCNT-exposed mice (Fig. 2B-D). The expression of *Esr1* was significantly reduced in Mitsui MWCNT-exposed mice compared to time-point matched control mice after 4 and 12 days of exposure. Expression of *Esr1* was reduced compared to controls after 2 and 8 days of exposure but the differences were not significant ($p > 0.05$, Fig. 2B). The expression of *Esr2* was significantly reduced compared to controls after 2 and 4 days and there was a trend of reduced expression at 8- and 12-days post exposure, but the differences were not significant ($p > 0.05$, Fig. 2). *Gper1* mRNA expression varied the most and the relative expression levels inverted over the time-course and were only significantly different ($p < 0.05$) after 4 days of exposure (Fig. 2D).

### 3.4. ESR1 is expressed in hyperplastic and hypertrophic bronchiolar epithelial cells and inflammatory macrophages in vivo

Next, we sought to localize ESR1 antigen expression in lungs of animals exposed to MWCNTs by immunohistochemistry. We focused on ESR1 because we observed the largest change in *Esr1* mRNA expression in the lungs of mice exposed to MWCNTs and its baseline mRNA expression was greater than *Esr2* (Fig. 2). Results showed nuclear expression of ESR1 antigen in hyperplastic/hypertrophic bronchiolar epithelial cells, but staining was also prominent in inflammatory macrophages that were often associated with engulfed deposits of particles (Fig. 3).

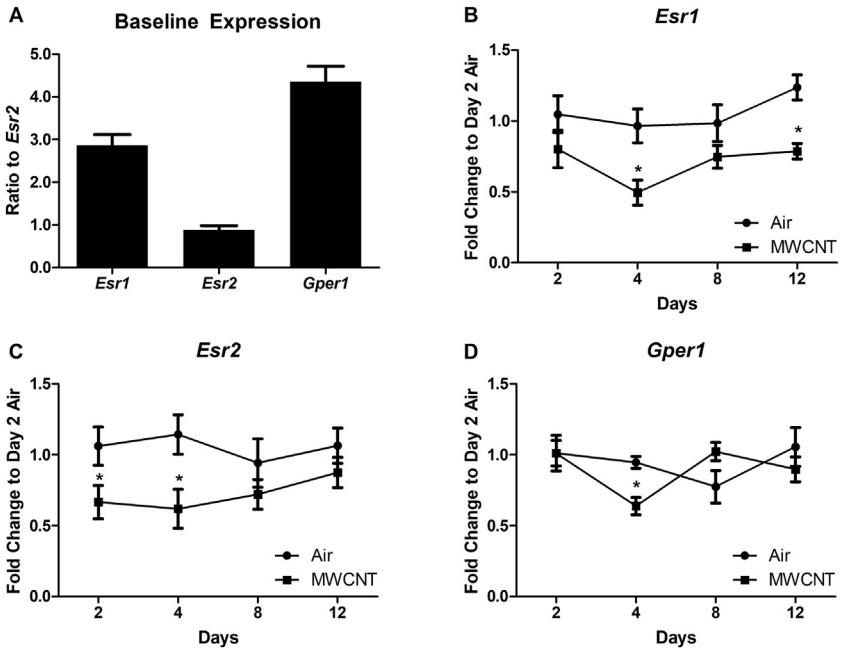


**Fig. 2.** Mitsui MWCNTs reduce estrogen receptor expression in mouse lungs. A) *Esr* gene expression was normalized to *Gapdh* mRNA expression and calculated as a ratio to *Esr2* mRNA expression as described in (Pfaffl, 2001). Relative baseline expression levels of each estrogen receptor in whole lung tissue of mice exposed to clean air for two days ($n = 8$) was *Gper1* > *Esr1* > *Esr2*. Mice were exposed by whole body inhalation to clean air for 2, 4, 8, or 12 days (n = 8, 8, 6, 8, respectively) or 10 mg/m$^3$ aerosolized Mitsui MWCNTs for 5 h per day for 2, 4, 8, or 12 days ($n = 9$, 7, 5, and 6, respectively) and expression of B) *Esr1*, C) *Esr2*, and D) *Gper1* was determined by qPCR, normalized to *Gapdh*, and fold change calculated by relative ΔΔCq method. Data are mean ± SEM of mRNA expression relative to day 2 control mice. Asterisks (*) indicate statistically significant ($p < 0.05$) differences from control at each time-point as determined by two-tailed, unpaired *t*-test.

### 3.5. Mitsui MWCNTs reduce ESR1 mRNA expression in BEAS-2Bs

To begin mechanistic evaluations of a role for TGF-β1 in MWCNT-induced repression of estrogen receptor mRNA expression, we characterized the response in bronchial epithelial cells (BEAS-2Bs) *in vitro*. First, we measured the relative baseline expression levels of *ESR1*, *ESR2*, and *GPER1* in control cells as a ratio to *ESR2* using the method described previously (Pfaffl, 2001). The expression pattern for each receptor subtype *in vitro* was *GPER1* > *ESR1* > *ESR2* which matched the relative pattern observed in mouse lungs *in vivo* (Fig. 4A).

Similar to results observed *in vivo*, exposure of BEAS-2Bs to Mitsui MWCNTs (0.2, 2, and 20 μg/mL) for 48 h significantly reduced *ESR1* mRNA expression (Fig. 4B) but did not significantly impact *GPER1* mRNA expression (Fig. 4D). In contrast to the *in vivo* results, *in vitro* exposure to Mitsui MWCNTs did not affect *ESR2* expression (Fig. 4C). Interestingly, exposure to Helix MWCNTs which are also pristine (non-surface functionalized) did not reduce *ESR1* mRNA expression *in vitro* in BEAS-2Bs (Supplementary Fig. 2) despite similar physiochemical properties (*i.e.* width, HDR, Supplementary Fig. 3) and ROS production (Supplementary Fig. 4).

### 3.6. Mitsui MWCNTs reduce ESR1 mRNA expression in a TGF-β1-dependent manner in BEAS-2Bs

To determine whether TGF-β1 mediated the Mitsui MWCNT-induced reduction in *ESR1* mRNA expression *in vitro*, we used a selective inhibitor of TGF-β type-I receptor (TBRI), LY 364947, to block TGF-β1-mediated signaling. Cells were pre-treated with 20 μM LY 364947 for 2 h, then exposed to 20 μg/mL Mitsui MWCNTs for 48 h in the presence or absence of 20 μM LY 364947. As before, exposure of cells to Mitsui MWCNTs significantly reduced *ESR1* mRNA expression, and treatment with LY 364947 inhibited this response (Fig. 5B).

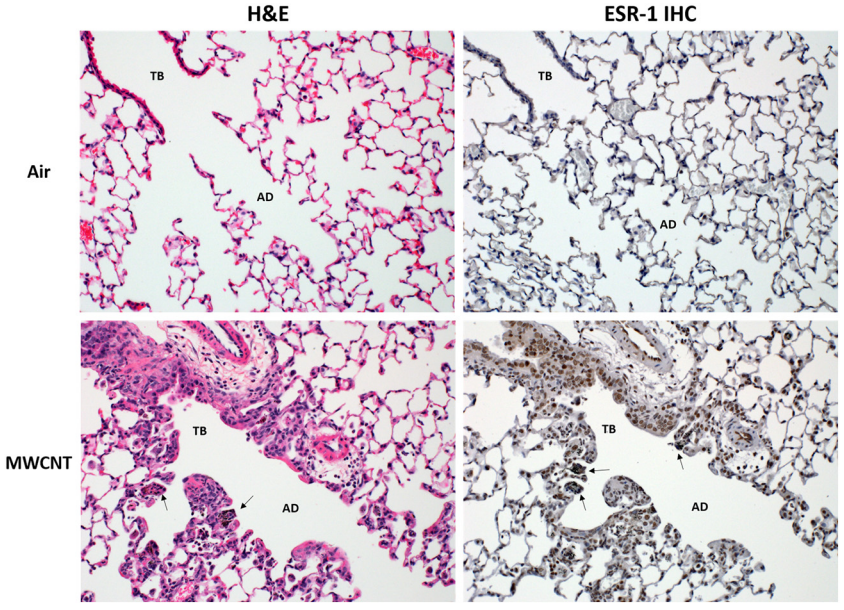


**Fig. 3.** Photomicrographs (20× magnification) of lung sections from mice exposed to air or MWCNT for 8 days that were stained with hematoxylin and eosin (H&E) or immunohistochemistry for estrogen receptor-1 (ESR-1). Epithelial hyperplasia and hypertrophy are seen at terminal bronchioles (TB) in MWCNT-exposed mice. Increased numbers of inflammatory macrophages often containing black particles (arrows), are present at the alveolar duct (AD) extending into adjacent alveoli. IHC for ESR-1 demonstrated nuclear staining of hyperplastic/hypertrophic bronchiolar epithelial cells and inflammatory macrophages. Air-exposed murine lung shows normal pulmonary architecture.

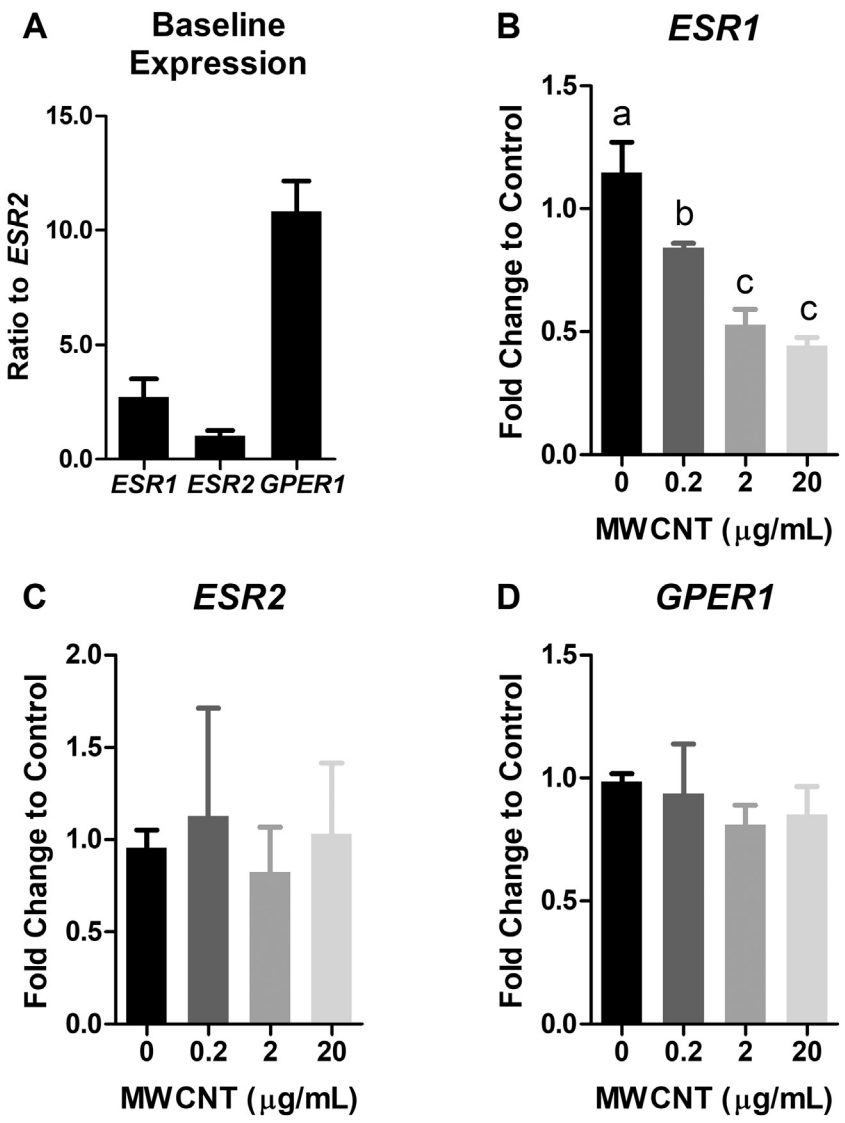


**Fig. 4.** Mitsui MWCNTs reduce expression of *ESR1* but not *ESR2* or *GPER1* mRNA expression in BEAS-2Bs. A) ESR gene expression was normalized to *GAPDH* mRNA expression and calculated as a ratio to *ESR2* mRNA expression as described in (Pfaffl, 2001). Relative baseline expression levels of each receptor in control cells was *GPER1* > *ESR1* > *ESR2*. (B-D) BEAS-2Bs were exposed to increasing concentrations of Mitsui MWCNTs for 48 h and expression of B) *ESR1*, C) *ESR2*, and D) *GPER1* was measured by qPCR, normalized to *GAPDH*, and fold change calculated by relative ΔΔCq method. Data are mean ± SEM of three independent experiments. Letters indicate statistically significant ($p < 0.05$) differences as determined by one-way ANOVA followed by Newman-Keuls multiple comparison test.

## 4. Discussion

MWCNT use is rapidly growing which raises concern for potential adverse health effects through inhalation exposures, including the development of pulmonary fibrosis. There is extensive evidence in small animal models that MWCNTs cause fibrotic like changes in the lung (Vietti et al., 2016), but limited studies have probed a role for steroid signaling despite epidemiological data indicating sex-specific trends in the incidence, prevalence, and survival rates of IPF (Han et al., 2008) and studies in animal models indicating sex-specific differences in pulmonary fibrotic responses (Gharaee-Kermani et al., 2005; Lekgabe et al., 2006; Voltz et al., 2008; Redente et al., 2011). As such, the purpose of this work was to begin investigations into interactions between pro-fibrogenic signaling and estrogen receptors in a model of MWCNT-induced fibrosis, to highlight a potential role for estrogen signaling in the fibrogenic response, which could be used to direct more extensive studies to probe sex differences and molecular mechanisms of action that involve ESRs. Through a combination of *in vivo* and *in vitro* exposure studies, we highlight *Esr1* and *Esr2* mRNA expression as targets of Mitsui MWCNT-induced signaling in mouse lungs *in vivo*, and *ESR1* mRNA expression as a target in human lung cells *in vitro*. We proceed to show that the inhibitory effect of MWCNTs on *ESR1* expression is mediated by TGF-β1. This work is the first to support estrogen receptors as targets of pro-fibrogenic signaling induced by MWCNT which may influence lung function regulated by E2.

As TGF-β1 is a well-established driver of extracellular matrix deposition and fibrosis in the lung, particularly in MWCNT-induced fibrogenesis (Wang et al., 2013; Mishra et al., 2015), we measured TGF-β1 levels in the BALF of Mitsui MWCNT-exposed mice. Similar to previous studies (Wang et al., 2011; Ronzani et al., 2012; Li et al., 2013; Wang et al., 2013; Chen et al., 2014; Dong et al., 2015), exposure to MWCNTs resulted in a trend of increased TGF-β1 levels in the BALF of mice exposed to Mitsui MWCNTs in this study (Fig. 1). The lower induction of TGF-β1 in our study is likely due to the time-point analyzed. A previous study reported induction of TGF-β1 in the BALF of mice exposed to a similar dose (4 mg/m$^3$) and type (rigid) of MWCNT although their levels were higher (and significant), but the time point was 21 days post exposure (Duke et al., 2017). Our increased trend of TGF-β1 at 4 days post exposure is possibly capturing the initial response. Future studies should include a comprehensive time-course analysis of TGF-β1 in the BALF of mice exposed to 10 mg/m$^3$ for 5 h per day to better correlate BALF TGF-β1 levels with reduced estrogen receptor expression in the lung observed in this study. Importantly, the dose of MWCNTs used in the studies described herein (5–10 mg/m$^3$ for 5 h per day) is occupationally-relevant given that mice exposed for four days to 10 mg/m$^3$ MWCNTs for 5 h per day approximates human deposition for a person performing light work for approximately 27–103 months based on analysis of total lung burden (Porter et al., 2012).

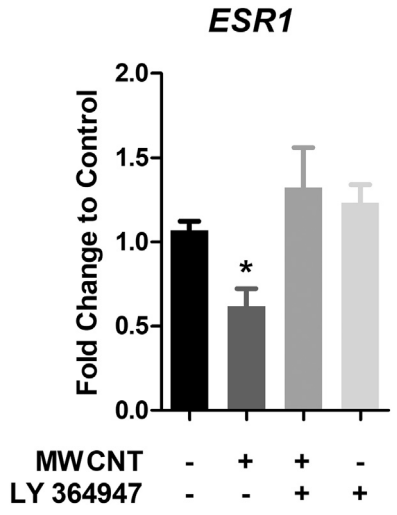


**Fig. 5.** Mitsui MWCNT-induced reduction of *ESR1* mRNA expression is partly dependent on TGF-β1 signaling. BEAS-2B cells were exposed to TGF-β1 inhibitor (20 μM LY 364947) for 2 h, then exposed to 20 μg/mL Mitsui MWCNTs in the presence or absence of 20 μM LY 364947 for 48 h. *ESR1* mRNA expression was measured by qPCR, normalized to *GAPDH*, and fold change calculated by relative ΔΔCq method. Data are mean ± SEM of three independent experiments. Asterisks (*) indicate significant differences ($p < 0.05$) compared to control as determined by a two-tailed, unpaired *t*-test.

There is a growing body of evidence suggesting that carbon-based nanoparticles are capable of interfering with endocrine signaling in reproductive tissues [reviewed by Iavicoli et al. (Iavicoli et al., 2013)]. However, few studies have focused on effects of particulate exposure on sex hormone regulation and signaling in non-reproductive organs and *vice versa*. This is despite evidence suggesting that sex hormones, particularly estrogen, play a role in lung physiology and disease (Carey et al., 2007a, 2007b; Tam et al., 2011; Shim et al., 2013). We characterized the effect of Mitsui MWCNT exposure on *Esr1*, *Esr2*, and *Gper1* mRNA expression in the mouse lung to infer a role for Mitsui MWCNTs in modulating E2 signaling in the lung. We found that *Esr1* and *Esr2* mRNA expression was reduced in the lungs of Mitsui MWCNT-exposed mice compared to controls at all time points, although the greatest reduction was for *Esr1* (Fig. 2B-C), whereas expression of *Gper1* was less affected (Fig. 2D). These data are consistent with a study which found that intratracheal instillation of silica nanoparticles to male and female mice significantly reduced *Esr1* and *Esr2* but not *Gper1* mRNA expression in lung tissue after 14 days (Brass et al., 2010). Using immunohistochemistry we were able to localize ESR1 in epithelial cells but also noted positive staining in macrophages (Fig. 3). The levels of ESR1 protein was difficult to quantify but the expression in macrophages is consistent with previous reports detailing estrogenic responses of lung macrophages in the lung that are ESR1 specific (Keselman et al., 2017). We focused on ESR1 protein detection since this receptor type showed the most significant change at the mRNA level and good working antibodies were available (positive staining on reproductive tissues – data not shown). Certainly, a more detailed time-course may shed additional opportunities to improve our quantitative ability but these results do show that several cell types, including epithelial cells, express ESR1.

To begin mechanistic investigations into pathways contributing to the MWCNT-induced repression of estrogen receptor mRNA, we sought to develop an *in vitro* system that would allow us to more easily probe potential signaling pathways. We chose BEAS-2Bs because we observed positive immunostaining of ESR1 in bronchial cells in the mouse lung (Fig. 3) and they exhibited a similar estrogen receptor expression profile (Fig. 4A). We determined that only *ESR1* mRNA expression exhibited a dose-dependent reduction in expression following MWCNT exposure (Fig. 4B-D) contrary to the *in vivo* results where all the receptor's mRNA levels were reduced. Based on alveolar surface area of mice ($0.05\ m^2$) the calculated dose to the alveolar surface *in vivo* is between the comparable low and medium doses we employed in the *in vitro* studies and therefore differences in dosimetry do not seem like a major contributing factor. However, it is important to note that the *in vivo* responses were observed in whole lung tissue and therefore we cannot determine which cell types are driving the response *in vivo*. This is supported by our immunohistochemistry data which clearly show other cells types are contributing.

It is well known that subtle differences in nanoparticle dimension and structure can drastically influence their behavior in biological systems and their ability to alter biological responses (Grabinski et al., 2007; Manke et al., 2013). As such, we questioned whether the responses observed in our study were specific to Mitsui MWCNTs. We chose to focus our studies primarily on exposure to Mitsui nanotubes because they are considered 'more pathogenic' than other types – which is a major reason for their declining manufacture and use – although conflicting data still exists. Data generated from exposure to these particular nanotubes allows us to benchmark our estrogen responses against a well published type of nanotube with respect to pulmonary injury and disease (*i.e.* fibrosis). Helix MWCNTs are similar to Mitsui MWCNTs with respect to surface chemistry (pristine non-surface functionalized) individual nanotube width (~40–50 nm) and length (range 1–13 μm; average 5 μm) and both show a consistent ability to produce ROS (Supplementary Fig. 4). Yet Helix MWCNTs did not reduce *ESR1* mRNA expression (Supplementary Fig. 2). This suggests other properties or behavior is driving the varied repression of ESR1. The evolution of HDR in cell culture media was measured for 48 h and did not differ drastically although the mean HDR for Helix were smaller (469 nm) compared to Mitsui (546 nm) nanotubes. The overall range was large which can be attributed to heterogeneous dispersion of the MWNTs in the cell culture media. Both types of nanotubes were dispersed in the media in their pristine form and the high van der Waals attraction force between MWCNT bundles is a primary reason for such heterogeneity. Interestingly, Mitsui nanotubes seemed more unstable over time (Supplementary Fig. 3). Of note, the variable responses are likely not due to surface properties as a recent report showed that changing the surface chemistry of Helix tubes (coating with $AL_2O_3$) had little effect on pulmonary responses including inflammation and proteomic changes compared to the same uncoated particles (Hilton et al., 2015; Rahman et al., 2017). The most striking differences between the two nanotubes is in their reported rigidity; Mitsui MWCNTs are known as extremely rigid nanotubes and are described as having high crystallinity (Nagai et al., 2011). It is possible that the slight differences in stability, agglomerate size and rigidity between the MWCNTs influence the dichotomous effects on *ESR1* mRNA expression.

We questioned whether TGF-β1 induction could drive Mitsui MWCNT-induced inhibition of ESR1 mRNA expression. We found that LY 364947, the TBR1 inhibitor, rescued *ESR1* expression in the presence of Mitsui MWCNTs suggesting that the inhibitory effects were at least partly mediated through TGF-β1 (Fig. 5). It has been previously shown that Mitsui MWCNTs increase TGF-β1 production in lung epithelial and fibroblast cells *in vitro* while helical types (like Helix) failed to do so (Vietti et al., 2013). These data collectively suggest that Mitsui MWCNTs specifically influence *ESR1* expression through modulation of TGF-β1. Direct interactions between TGF-β1 and estrogen receptor signaling have been previously reported by a few studies, however most of these have focused on reproductive cancer models (Stoica et al., 1997; Petrel and Brueggemeier, 2003; Mak et al., 2010; Fridriksdottir et al., 2015). Only two studies have examined interactions between TGF-β1 and estrogen receptor signaling in the lung, including one which showed that E2 exposure increased TGF-β1 expression in lung fibroblasts isolated from rats exposed to bleomycin (Gharaee-Kermani et al., 2005), a result that would seem to contribute to fibrosis rather than repress related signaling. Another study found that exogenous

TGF-β1 administration resulted in reduced estrogen receptor expression in bronchial epithelial cells (Smith et al., 2018). Furthermore, TGF-β1 is known to be produced by several cell types (Pociask et al., 2004; Fernandez and Eickelberg, 2012) that we also now show to contain detectable levels of ESR1, including epithelial cells and macrophages. How these cell types, steroids and pro-fibrotic pathways influence particle-induced lung injury is a next logical step of investigation.

The novel observation that Mitsui MWCNT-induced reduction in *Esr1* and *Esr2* mRNA expression *in vivo* and *ESR1* mRNA expression *in vitro* begs the question of whether there are potential adverse biological effects associated with this phenomenon. ERs are known to influence lung development (Patrone et al., 2003; Massaro and Massaro, 2004; Massaro and Massaro, 2006), but perhaps more relevant to this study, are the effects of E2 through ESR1 on a variety of respiratory parameters in adult mice including breathing and respiratory rhythmogenesis (Carey et al., 2007a, 2007b). A recent study reported that E2 regulated the expression of genes involved in chromatin remodeling, epigenetic modification of histones, and vasodilation in lung cells (Smith et al., 2018). Further, transgenic mice lacking ESR1 exhibited increased airway hyperresponsiveness to inhaled methacholine compared to wildtype mice (Carey et al., 2007a, 2007b), and another study using transgenic mice lacking ESR2 found that the protective effects of E2 on lung injury after trauma-hemorrhage were mediated by ESR2 (Toth et al., 2003). In addition, a role for sex steroids in lung function, including response to stressors, is now recognized and is postulated to be an important player in the sex differences observed for several other lung diseases (asthma, COPD, cancer) (Fuseini and Newcomb, 2017; Keselman et al., 2017; Słowikowski et al., 2017). However, the consequence of reduced estrogen receptor expression on the development or progression of fibrosis is less defined.

In conclusion, we observed a previously unreported interaction between Mitsui MWCNT-induced signaling and estrogen receptors that was at least partially mediated through induction of TGF-β1. Collectively, this work suggests Mitsui MWCNTs disrupt estrogen signaling in the lung; however, it remains to be determined whether the reduced estrogen receptor mRNA expression influences the fibrotic response to MWCNTs or whether this represents an off-target effect with added consequences on lung function.

## Conflict of interest

The authors declare that they have no competing interests.

## Author contributions

L.C.S. and T.S.A. conceived the study and designed the experiments. L.C.S., S.M., L.R., S.R, M.O., and D.D. performed the experiments. L.C.S., M.O., D.W. P., D.D., N.B.S., and T.S.A. interpreted the results. L.C.S. drafted the manuscript and T.S.A. edited. L.C.S., S.M., L.R., S.R., M.O., D.W.P., D.D., N.B.S., and T.S.A. approved the final version of the manuscript.

## Disclaimer

The findings and conclusions in this report are those of the authors and do not necessarily represent the official position of the National Institute for Occupational Safety and Health, Centers for Disease Control and Prevention.

## Funding

This work was supported by the National Institutes of Health (R01HL114907 to TSA).

## Appendix A. Supplementary data

Supplementary data to this article can be found online at https://doi.org/10.1016/j.impact.2019.100152.

## References

Beck, L.A., Tancowny, B., Brummet, M.E., Asaki, S.Y., Curry, S.L., Penno, M.B., Foster, M., Bahl, A., Stellato, C., 2006. Functional analysis of the chemokine receptor CCR3 on airway epithelial cells. J. Immunol. 177 (5), 3344–3354.
Brass, D.M., McGee, S.P., Dunkel, M.K., Reilly, S.M., Tobolewski, J.M., Sabo-Attwood, T., Fattman, C.L., 2010. Gender influences the response to experimental silica-induced lung fibrosis in mice. Am J Physiol Lung Cell Mol Physiol 299 (5), L664–L671.
Carey, M.A., Card, J.W., Voltz, J.W., Arbes, S.J., Germolec, D.R., Korach, K.S., Zeldin, D.C., 2007a. It's all about sex: gender, lung development and lung disease. Trends Endocrinol. Metab. 18 (8), 308–313.
Carey, M.A., Card, J.W., Voltz, J.W., Germolec, D.R., Korach, K.S., Zeldin, D.C., 2007b. The impact of sex and sex hormones on lung physiology and disease: lessons from animal studies. Am J Physiol Lung Cell Mol Physiol 293 (2), L272–L278.
Chen, T., Nie, H., Gao, X., Yang, J., Pu, J., Chen, Z., Cui, X., Wang, Y., Wang, H., Jia, G., 2014. Epithelial–mesenchymal transition involved in pulmonary fibrosis induced by multi-walled carbon nanotubes via TGF-beta/Smad signaling pathway. Toxicol. Lett. 226 (2), 150–162.
De Volder, M.F., Tawfick, S.H., Baughman, R.H., Hart, A.J., 2013. Carbon nanotubes: present and future commercial applications. Science 339 (6119), 535–539.
Donaldson, K., Poland, C.A., Murphy, F.A., MacFarlane, M., Chernova, T., Schinwald, A., 2013. Pulmonary toxicity of carbon nanotubes and asbestos - similarities and differences. Adv. Drug Deliv. Rev. 65.
Dong, J., Porter, D.W., Batteli, L.A., Wolfarth, M.G., Richardson, D.L., Ma, Q., 2015. Pathologic and molecular profiling of rapid-onset fibrosis and inflammation induced by multi-walled carbon nanotubes. Arch. Toxicol. 89 (4), 621–633.
Duke, K.S., Taylor-Just, A.J., Ihrie, M.D., Shipkowski, K.A., Thompson, E.A., Dandley, E.C., Parsons, G.N., Bonner, J.C., 2017. STAT1-dependent and-independent pulmonary allergic and fibrogenic responses in mice after exposure to tangled versus rod-like multi-walled carbon nanotubes. Part Fibre Toxicol 14 (1), 26.
Endo, M., Strano, M., Ajayan, P., 2008. Potential applications of carbon nanotubes. Carbon nanotubes 13–61.
Fatkhutdinova, L.M., Khaliullin, T.O., Vasil'yeva, O.L., Zalyalov, R.R., Mustafin, I.G., Kisin, E.R., Birch, M.E., Yanamala, N., Shvedova, A.A., 2016. Fibrosis biomarkers in workers exposed to MWCNTs. Toxicol. Appl. Pharmacol. 299, 125–131.
Fernandez, I.E., Eickelberg, O., 2012. The impact of TGF-β on lung fibrosis: from targeting to biomarkers. Proc. Am. Thorac. Soc. 9 (3), 111–116.
Filardo, E.J., Quinn, J.A., Frackelton Jr., A.R., Bland, K.I., 2002. Estrogen action via the G protein-coupled receptor, GPR30: stimulation of adenylyl cyclase and cAMP-mediated attenuation of the epidermal growth factor receptor-to-MAPK signaling axis. Mol. Endocrinol. 16 (1), 70–84.
Fridriksdottir, A.J., Kim, J., Villadsen, R., Klitgaard, M.C., Hopkinson, B.M., Petersen, O.W., Rønnov-Jessen, L., 2015. Propagation of oestrogen receptor-positive and oestrogen-responsive normal human breast cells in culture. Nat. Commun. 6, 8786.
Fuseini, H., Newcomb, D.C., 2017. Mechanisms driving gender differences in asthma. Curr Allergy Asthma Rep 17 (3), 19.
Gharaee-Kermani, M., Hatano, K., Nozaki, Y., Phan, S.H., 2005. Gender-based differences in bleomycin-induced pulmonary fibrosis. Am. J. Pathol. 166 (6), 1593–1606.
Grabinski, C., Hussain, S., Lafdi, K., Braydich-Stolle, L., Schlager, J., 2007. Effect of particle dimension on biocompatibility of carbon nanomaterials. Carbon 45 (14), 2828–2835.
Gribbin, J., Hubbard, R.B., Le Jeune, I., Smith, C.J., West, J., Tata, L.J., 2006. Incidence and mortality of idiopathic pulmonary fibrosis and sarcoidosis in the UK. Thorax 61 (11), 980–985.
Gruber, C.J., Tschugguel, W., Schneeberger, C., Huber, J.C., 2002. Production and actions of estrogens. New Engl J Med 346 (5), 340–352.
Ha, J., Choi, H.S., Lee, Y., Kwon, H.J., Song, Y.W., Kim, H.H., 2010. CXC chemokine ligand 2 induced by receptor activator of NF-κB ligand enhances osteoclastogenesis. J. Immunol. 184 (9), 4717–4724.
Han, M.K., Murray, S., Fell, C.D., Flaherty, K.R., Toews, G.B., Myers, J., Colby, T.V., Travis, W.D., Kazerooni, E.A., Gross, B.H., Martinez, F.J., 2008. Sex differences in physiological progression of idiopathic pulmonary fibrosis. Eur. Respir. J. 31 (6), 1183–1188.
Hellemans, J., Mortier, G., De Paepe, A., Speleman, F., Vandesompele, J., 2007. qBase relative quantification framework and software for management and automated analysis of real-time quantitative PCR data. Genome Biol. 8 (2), R19.
Hilton, G.M., Taylor, A.J., McClure, C.D., Parsons, G.N., Bonner, J.C., Bereman, M.S., 2015. Toxicoproteomic analysis of pulmonary carbon nanotube exposure using LC-MS/MS. Toxicology 329, 80–87.
Iavicoli, I., Fontana, L., Leso, V., Bergamaschi, A., 2013. The effects of nanomaterials as endocrine disruptors. Int. J. Mol. Sci. 14 (8), 16732–16801.
Keselman, A., Fang, X., White, P.B., Heller, N.M., 2017. Estrogen signaling contributes to sex differences in macrophage polarization during asthma. J. Immunol. 199 (5), 1573–1583.
Lekgabe, E.D., Royce, S.G., Hewitson, T.D., Tang, M.L.K., Zhao, C., Moore, X.L., Tregear, G.W., Bathgate, R.A., Du, X.J., Samuel, C.S., 2006. The effects of relaxin and estrogen deficiency on collagen deposition and hypertrophy of nonreproductive organs. Endocrinology 147 (12), 5575–5583.
Li, R., Wang, X., Ji, Z., Sun, B., Zhang, H., Chang, C.H., Lin, S., Meng, H., Liao, Y.P., Wang,

M., 2013. Surface charge and cellular processing of covalently functionalized multiwall carbon nanotubes determine pulmonary toxicity. ACS Nano 7 (3), 2352–2368.
Mak, P., Leav, I., Pursell, B., Bae, D., Yang, X., Taglienti, C.A., Gouvin, L.M., Sharma, V.M., Mercurio, A.M., 2010. ERβ impedes prostate cancer EMT by destabilizing HIF-1α and inhibiting VEGF-mediated snail nuclear localization: implications for Gleason grading. Cancer Cell 17 (4), 319–332.
Manke, A., Wang, L., Rojanasakul, Y., 2013. Mechanisms of nanoparticle-induced oxidative stress and toxicity. Biomed. Res. Int. 2013, 15.
Massaro, D., Massaro, G.D., 2004. Estrogen regulates pulmonary alveolar formation, loss, and regeneration in mice. Am J Physiol Lung Cell Mol Physiol 287 (6), L1154–L1159.
Massaro, D., Massaro, G.D., 2006. Estrogen receptor regulation of pulmonary alveolar dimensions: alveolar sexual dimorphism in mice. Am J Physiol Lung Cell Mol Physiol 290 (5), L866–L870.
Mercer, R.R., Scabilloni, J.F., Hubbs, A.F., Battelli, L.A., McKinney, W., Friend, S., Wolfarth, M.G., Andrew, M., Castranova, V., Porter, D.W., 2013. Distribution and fibrotic response following inhalation exposure to multi-walled carbon nanotubes. Part Fibre Toxicol 10 (1), 33.
Mishra, A., Stueckle, T.A., Mercer, R.R., Derk, R., Rojanasakul, Y., Castranova, V., Wang, L., 2015. Identification of TGF-β receptor-1 as a key regulator of carbon nanotube-induced fibrogenesis. Am J Physiol Lung Cell Mol Physiol 309 (8), L821–L833.
Muller, J., Huaux, F., Moreau, N., Misson, P., Heilier, J.F., Delos, M., Arras, M., Fonseca, A., Nagy, J.B., Lison, D., 2005. Respiratory toxicity of multi-wall carbon nanotubes. Toxicol. Appl. Pharmacol. 207 (3), 221–231.
Nagai, H., Okazaki, Y., Chew, S.H., Misawa, N., Yamashita, Y., Akatsuka, S., Ishihara, T., Yamashita, K., Yoshikawa, Y., Yasui, H., 2011. Diameter and rigidity of multiwalled carbon nanotubes are critical factors in mesothelial injury and carcinogenesis. Proc. Natl. Acad. Sci. U. S. A. 108 (49), E1330–E1338.
Patrone, C., Cassel, T.N., Pettersson, K., Piao, Y.S., Cheng, G., Ciana, P., Maggi, A., Warner, M., Gustafsson, J.Å., Nord, M., 2003. Regulation of postnatal lung development and homeostasis by estrogen receptor β. Mol. Cell. Biol. 23 (23), 8542–8552.
Petrel, T.A., Brueggemeier, R.W., 2003. Increased proteasome-dependent degradation of estrogen receptor-alpha by TGF-β1 in breast cancer cell lines. J. Cell. Biochem. 88 (1), 181–190.
Pfaffl, M.W., 2001. A new mathematical model for relative quantification in real-time RT–PCR. Nucleic Acids Res. 29 (9), e45.
Pociask, D.A., Sime, P.J., Brody, A.R., 2004. Asbestos-derived reactive oxygen species activate TGF-β1. Lab. Investig. 84 (8), 1013–1023.
Poland, C.A., Duffin, R., Kinloch, I., Maynard, A., Wallace, W.A.H., Seaton, A., Stone, V., Brown, S., MacNee, W., Donaldson, K., 2008. Carbon nanotubes introduced into the abdominal cavity of mice show asbestos-like pathogenicity in a pilot study. Nat. Nanotechnol. 3 (7), 423–428.
Porter, D., Sriram, K., Wolfarth, M., Jefferson, A., Schwegler-Berry, D., Andrew, M.E., Castranova, V., 2008. A biocompatible medium for nanoparticle dispersion. Nanotoxicology 2 (3), 144–154.
Porter, D.W., Hubbs, A.F., Chen, B.T., McKinney, W., Mercer, R.R., Wolfarth, M.G., Battelli, L., Wu, N., Sriram, K., Leonard, S., 2012. Acute pulmonary dose–responses to inhaled multi-walled carbon nanotubes. Nanotoxicology 7 (7), 1179–1194.
Prossnitz, E.R., Arterburn, J.B., Smith, H.O., Oprea, T.I., Sklar, L.A., Hathaway, H.J., 2008. Estrogen signaling through the transmembrane G protein–coupled receptor GPR30. Annu. Rev. Physiol. 70, 165–190.
Rahman, L., Jacobsen, N.R., Aziz, S.A., Wu, D., Williams, A., Yauk, C.L., White, P., Wallin, H., Vogel, U., Halappanavar, S., 2017. Multi-walled carbon nanotube-induced genotoxic, inflammatory and pro-fibrotic responses in mice: investigating the mechanisms of pulmonary carcinogenesis. Mutat. Res. Genet. Toxicol. Environ. Mutagen. 823, 28–44.
Redente, E.F., Jacobsen, K.M., Solomon, J.J., Lara, A.R., Faubel, S., Keith, R.C., Henson, P.M., Downey, G.P., Riches, D.W., 2011. Age and sex dimorphisms contribute to the severity of bleomycin-induced lung injury and fibrosis. Am J Physiol Lung Cell Mol Physiol 301 (4), L510–L518.
Ronzani, C., Spiegelhalter, C., Vonesch, J.-L., Lebeau, L., Pons, F., 2012. Lung deposition and toxicological responses evoked by multi-walled carbon nanotubes dispersed in a synthetic lung surfactant in the mouse. Arch. Toxicol. 86 (1), 137–149.
Ryman-Rasmussen, J.P., Cesta, M.F., Brody, A.R., Shipley-Phillips, J.K., Everitt, J.I., Tewksbury, E.W., Moss, O.R., Wong, B.A., Dodd, D.E., Andersen, M.E., 2009a. Inhaled carbon nanotubes reach the subpleural tissue in mice. Nat. Nanotechnol. 4 (11), 747–751.
Sargent, L.M., Porter, D.W., Staska, L.M., Hubbs, A.F., Lowry, D.T., Battelli, L., 2014. Promotion of lung adenocarcinoma following inhalation exposure to multi-walled carbon nanotubes. Part Fibre Toxicol 11.
Sathish, V., Martin, Y.N., Prakash, Y.S., 2015. Sex steroid signaling: implications for lung diseases. Pharmacol. Ther. 150, 94–108.
Shim, B., Pacheco-Rodriguez, G., Kato, J., Darling, T.N., Vaughan, M., Moss, J., 2013. Sex-specific lung diseases: effect of oestrogen on cultured cells and in animal models. Eur. Respir. Rev. 22 (129), 302–311.
Słowikowski, B.K., Lianeri, M., Jagodziński, P.P., 2017. Exploring estrogenic activity in lung cancer. Mol. Biol. Rep. 44 (1), 35–50.
Smith, L.C., Moreno, S., Robertson, L., Robinson, S., Gant, K., Bryant, A.J., Sabo-Attwood, T., 2018. Transforming growth factor beta1 targets estrogen receptor signaling in bronchial epithelial cells. Respir. Res. 19 (1), 160.
Spizzo, R., Nicoloso, M., Lupini, L., Lu, Y., Fogarty, J., Rossi, S., Zagatti, B., Fabbri, M., Veronese, A., Liu, X., 2010. miR-145 participates with TP53 in a death-promoting regulatory loop and targets estrogen receptor-α in human breast cancer cells. Cell Death Differ. 17 (2), 246–254.
Stoica, A., Saceda, M., Fakhro, A., Solomon, H.B., Fenster, B.D., Martin, M.B., 1997. The role of transforming growth factor-β in the regulation of estrogen receptor expression in the MCF-7 breast cancer cell line. Endocrinology 138 (4), 1498–1505.
Tam, A., Morrish, D., Wadsworth, S., Dorscheid, D., Man, S.P., Sin, D.D., 2011. The role of female hormones on lung function in chronic lung diseases. BMC Womens Health 11 (1), 24.
Toth, B., Schwacha, M.G., Kuebler, J.F., Bland, K.I., Wang, P., Chaudrya, I.H., 2003. Gender dimorphism in neutrophil priming and activation following trauma-hemorrhagic shock. Int. J. Mol. Med. 11 (3), 357–364.
Townsend, E.A., Miller, V.M., Prakash, Y., 2012. Sex differences and sex steroids in lung health and disease. Endocr. Rev. 33 (1), 1–47.
Vietti, G., Ibouraadaten, S., Palmai-Pallag, M., Yakoub, Y., Bailly, C., Fenoglio, I., Marbaix, E., Lison, D., van den Brule, S., 2013. Towards predicting the lung fibrogenic activity of nanomaterials: experimental validation of an in vitro fibroblast proliferation assay. Part Fibre Toxicol 10 (1), 52.
Vietti, G., Lison, D., van den Brule, S., 2016. Mechanisms of lung fibrosis induced by carbon nanotubes: towards an Adverse Outcome Pathway (AOP). Part Fibre Toxicol 13 (1), 11.
Voltz, J.W., Card, J.W., Carey, M.A., DeGraff, L.M., Ferguson, C.D., Flake, G.P., Bonner, J.C., Korach, K.S., Zeldin, D.C., 2008. Male sex hormones exacerbate lung function impairment after bleomycin-induced pulmonary fibrosis. Am. J. Respir. Cell Mol. Biol. 39 (1), 45–52.
Wang, X., Xia, T., Ntim, S.A., Ji, Z., George, S., Meng, H., Zhang, H., Castranova, V., Mitra, S., Nel, A.E., 2010. Quantitative techniques for assessing and controlling the dispersion and biological effects of multiwalled carbon nanotubes in mammalian tissue culture cells. ACS Nano 4 (12), 7241–7252.
Wang, X., Xia, T., Addo Ntim, S., Ji, Z., Lin, S., Meng, H., Chung, C.H., George, S., Zhang, H., Wang, M., 2011. Dispersal state of multiwalled carbon nanotubes elicits profibrogenic cellular responses that correlate with fibrogenesis biomarkers and fibrosis in the murine lung. ACS Nano 5 (12), 9772–9787.
Wang, P., Nie, X., Wang, Y., Li, Y., Ge, C., Zhang, L., Wang, L., Bai, R., Chen, Z., Zhao, Y., 2013. Multiwall carbon nanotubes mediate macrophage activation and promote pulmonary fibrosis through TGF-β/Smad signaling pathway. Small 9 (22), 3799–3811.
Wang, X., Duch, M.C., Mansukhani, N., Ji, Z., Liao, Y.-P., Wang, M., Zhang, H., Sun, B., Chang, C.H., Li, R., 2015. Use of a pro-fibrogenic mechanism-based predictive toxicological approach for tiered testing and decision analysis of carbonaceous nanomaterials. ACS Nano 9 (3), 3032–3043.
Ye, J., Coulouris, G., Zaretskaya, I., Cutcutache, I., Rozen, S., Madden, T.L., 2012. Primer-BLAST: a tool to design target-specific primers for polymerase chain reaction. BMC Bioinformatics 13 (1), 134.